SAE International

A Control Oriented Model with Variable Valve Timing for HCCI Combustion Timing Control

2013-01-0588
Published
04/08/2013

Khashayar Ebrahimi, Charles Koch and Alex Schramm
Univ of Alberta

doi:10.4271/2013-01-0588

ABSTRACT

Homogeneous Charge Compression Ignition (HCCI) is a promising concept for combustion engines to reduce both emissions and fuel consumption. HCCI combustion control is a challenging issue because there is no direct initiator of combustion. Variable Valve Timing (VVT) is being used in SI engines to improve engine efficiency. When VVT is used in conjunction with HCCI combustion it is an effective way to control the start of combustion. VVT changes the amount of trapped residual gas and the effective compression ratio for each cycle both of which have a strong effect on combustion timing in HCCI engines. To control HCCI combustion, a physics based control oriented model is developed that includes the effect of trapped residual gas on combustion timing. The control oriented model is obtained by taking a physics based model of the reaction kinetics and transient dynamics and systematically reducing the model using simplification of reaction mechanisms. This method allows different fuels to be incorporated using a standard methodology. The reduced order model consists of these five stages: intake, compression, combustion, expansion and exhaust. This model fills the gap between complex models with highly detailed chemical kinetics and simple black box dynamic models that have been used in model based control.

INTRODUCTION

Homogeneous charge compression ignition (HCCI) engines have the potential for high efficiencies and low pollutant emissions. HCCI engines are a combination of both conventional Spark Ignition (SI) and diesel Compression Ignition (CI) engines. In HCCI engines, fuel and air are homogeneously mixed and compressed similar to SI engines. When the piston is near to top dead center of the compression stroke, the air-fuel mixture auto-ignites at many locations. In order to control the rate of pressure rise in HCCI engines, the air and fuel mixture is diluted with burned gases. The combination of a diluted and premixed air fuel mixture with multiple ignition points inside the combustion chamber provides low temperature combustion zones that reduce the production of nitrogen oxides [1].

HCCI engines have no direct in-cylinder mechanism for combustion initiation, unlike the ignition event in SI and CI engines which are controlled by spark and fuel injection respectively. There are several ways to control the combustion timing in an HCCI engine. Intake air heating is one effective way for combustion timing control [2]. Usually, an electric air heater is used to raise the intake air temperature. This approach is not efficient because energy is required to heat the air and the heater response time is long compare to an engine cycle. Exhaust Gas Recirculation (EGR) is another way to control combustion timing. EGR has four effects [3, 4] but mainly increases the mixture temperature and dilutes the premixed charge [5, 6, 7, 8, 9, 10, 11, 12]. The combustion products can be retained or reinducted using Variable Valve Timing (VVT). This reduces heat loss and achieves fast control response compared to external EGR. Variable compression ratio engines can also be used to control the combustion timing [13, 14] but the mechanism is complex. Controlling the combustion timing by varying the autoignition properties of the fuel using dual-fuels is also effective but two fuels are needed [15, 16, 17]. Direct fuel injection is another way that can be used to control the auto ignition properties of the premixed charge [18, 19]. Water injection has also been used to cool the mixture and control the combustion timing in HCCI engines since the ignition timing is very temperature sensitive [20, 21].

HCCI combustion timing is controlled purely by chemical kinetics of the trapped charge [1, 22]. Therefore, to achieve ignition timing control of HCCI combustion, the mixture

composition, temperature and pressure at the Inlet Valve Closing (IVC) must be controlled. VVT enables quick changes in the amount of trapped hot residual gases inside the cylinder and is a simple and precise actuation method to set conditions at IVC for desired auto-ignition timing.

To implement closed-loop HCCI combustion timing control, a control oriented model is needed. Modeling has been found to be an important part of HCCI engine controller design. There are two main methods to obtain an HCCI control oriented model: physical [23, 24, 25] and system identification [15, 16, 26]. Physical models are classified according to the number of spatial dimensions in the cylinder, e.g. zero-dimensional [27, 28, 29, 30, 31] or computational fluid dynamics (three dimensional) models [32, 33, 34, 35]. Zero dimensional models provide no spatial resolution. Most of the zero-dimensional models are based on detailed chemical kinetics and are not suitable for control analysis. Computational fluid dynamics models are even more complex and usually produce only a single engine cycle of data. For control analysis, a model that is capable of quickly simulating many engine cycles is required.

Many HCCI engine models for control purposes have been developed [36, 37, 38]. In these models, the combustion mechanism is usually greatly simplified to decrease the simulation time. Ohyama [36] developed a real time physics based model for in-cylinder Air/Fuel ratio and trapped residual gas mass fraction estimation where air and residual gas mass fraction at the beginning of compression were determined based on signals from an air flow meter and in-cylinder pressure transducer. Shaver et. al. [37] developed a physical based control oriented model for a propane HCCI engine. An integrated Arrhe-nius rate expression was used to capture the importance of species concentrations and temperature on the ignition process. Rausen et. al. [39] developed a mean value model for the control of a HCCI engine. Their model has five continuous and three discrete states and the effects of exhaust gas recirculation and re-breathing was investigated. They used a simple Arrhenius integral model to estimate the start of combustion and algebraic equations were used for the heat release rate calculation. Ognik et. al. [38] developed a physics based model for a gasoline HCCI engine considering variable valve timing. Their model connected the SENKIN code of the CHEMKIN library [40] to the AVL BOOST [41] engine cycle simulation code and parametric studies of the combustion process in a single cylinder HCCI engine were described. Kara-giorgis et. al. [42] developed a simple non-linear low-order control oriented physical based model for a gasoline HCCI engine which is suitable for variable valve actuated HCCI engines. They used simple thermodynamics concepts to predict in-cylinder pressure and temperature at IVC. The gas exchange was based on in-cylinder dynamics and it was assumed that the manifold pressure is constant during gas exchange. Combustion was modeled in a semi empirical fashion. In [16], a system identification approach was used on a dual-fuel HCCI engine to generate input-output models for control. In [43], a control oriented model that simulates the engine cycle from the intake to the exhaust stroke including the thermal coupling dynamics caused by the residual gases from one cycle to the next cycle was developed. In their work, the gas exchange process, engine output work and combustion were predicted using semi-empirical correlations.

Despite extensive work on the modeling of HCCI combustion, to date no physical control oriented model can provide accurate and fast prediction of the combustion timing with the variation of trapped residual gas. Thus the focus of this work is to develop a control oriented model of HCCI combustion timing using a detailed physical based model.

DETAILED PHYSICAL MODEL (DPM)

A detailed HCCI four stroke cycle is modeled as a sequence of continuous processes: intake, compression, combustion, expansion and exhaust. In the cycle simulation, the system of interest is the instantaneous contents of a cylinder. This system is open to the transfer of mass, enthalpy and energy in the form of work and heat. The cylinder is modeled as a time variant volume and the cylinder contents are divided into fourteen continuous zones. Quasi steady, adiabatic, one dimensional flow equations are used to predict the mass flow past the intake and exhaust valves. The intake and exhaust manifolds are modeled as constant volumes whose pressure and temperature are determined by solving mass and energy equations for each manifold. Intake charge and exhaust gas are modeled as ideal gases. A reduced order reaction mechanism for n-heptane is used for combustion simulation. The reaction mechanism is from [44]. This reduced mechanism consists of 29 species and 52 reactions and is generated from the detailed n-heptane reaction mechanism [45].

Conservation of mass is used to develop a differential equation for the change in species concentration and energy conservation is used to obtain a differential equation for the change in system temperature. For the in-cylinder content, conservation of energy can be written [46] as:

$$\dot{U} = \sum_j \dot{m}_j h_j + \dot{Q}_W - \dot{W} \qquad (1)$$

where U is the internal energy, $\dot{Q}_W$ is the heat transfer rate into the system, $\dot{W}$ is the rate at which the system does work by boundary displacement and h_j is the enthalpy of the *jth* specie entering or leaving the system. The internal energy is calculated as the sum of the internal energies of all species

$$U = \sum_k m_k u_k \tag{2}$$

where *k* represents the zone number. Differentiating Equation 2 with respect to time gives

$$\dot{U} = \sum_k m_k \dot{u}_k + \sum_k \dot{m}_k u_k \tag{3}$$

For an ideal gas the change in internal energy can be written as:

$$\dot{u}_k = \bar{c_v} \dot{T}_k \tag{4}$$

The conservation of gas species in each zone can be calculated as:

$$\dot{y}_{k,j} = \frac{\dot{\omega}_{k,j} M_j}{\rho} + \sum_j \frac{\dot{m}_j}{m_{cyl}} (y_j - y_{cyl}) \tag{5}$$

where $\dot{\omega}_j$ is the net chemical production rate for each specie and M_j is the molar mass of each specie. Cantera [47] is used for the calculation of the net chemical production rate, internal energy and enthalpy of the gas species. Cantera is an open-source chemical kinetics software. The rate of change of mass in each zone is calculated as

$$\dot{m}_k = m_k \dot{y}_{k,j} \tag{6}$$

$\dot{W}$ in Equation 1 is calculated as

$$\dot{W} = P_{cyl} \dot{V}_k \tag{7}$$

where $\dot{V}_k$ and P_{cyl} are obtained from ideal gas law [27]

$$P_{cyl} = \frac{\sum_k m_k R_k T_k}{V_{cyl}} \tag{8}$$

$$\dot{V}_k = \dot{V}_{cyl} \frac{m_k R_k T_k}{\left(\sum_k m_k R_k \dot{T}_k\right)^2} \left(m_k R_k \dot{T}_k \sum_k m_k R_k T_k - m_k R_k T_k \sum_k m_k R_k \dot{T}_k\right) \tag{9}$$

The cylinder volume, as a function of engine crank angle θ, are calculated using the slider crank mechanism [48]

$$V_{cyl} = V_c + \frac{\pi B^2}{4} [l + a - a\cos\theta - \sqrt{l^2 - (a\sin\theta)^2}] \tag{10}$$

where V_c is the cylinder clearance volume, B is the cylinder bore, l is the connecting rod length and $L = 2a$ is the stroke.

The rate of change of temperature in each zone can be expressed by substituting Equations 3, 4, 5, 6, 7, 8, 9 into Equation 1, resulting in:

$$\dot{T}_k = \frac{1}{\bar{c_p}} \left(\sum_j \dot{m}_j h_j + \dot{Q} - \sum_j u_j \dot{y}_{k,j} + \frac{R_k T_k}{\sum_k m_k R_k T_k} \sum_k m_k R_k \dot{T}_k - \frac{R_k T_k}{V_{cyl}} \dot{V}_{cyl}\right) \tag{11}$$

The heat transfer rate between the cylinder wall and the adjacent zone is calculated using a convective heat transfer law. A slightly modified version of Woschni's correlation has shown good results for HCCI engines and is used here to determine the heat transfer coefficient [48]:

$$\dot{Q} = A_W h_c (T_{cyl} - T_{wall}) \tag{12}$$

$$h_c = 3.26 B^{-0.2} {p_{cyl}}^{0.8} {T_{cyl}}^{-0.55} \bar{n}^{0.8} \tag{13}$$

$$\bar{n} = C_1 \bar{S}_p \tag{14}$$

where A_W is the cylinder wall area available for heat transfer, h_c is the heat transfer coefficient, and T_{wall} is the in-cylinder wall surface temperature. C_1 is 6.18 during induction and exhaust and 2.28 otherwise. B is the cylinder bore and $\bar{S}_p$ is the mean piston speed. The heat transfer between each zones due to the temperature difference is calculated based on a simple conduction model developed in [27]. Residual gas mass and temperature distribution at IVC are obtained by the model proposed in [27].

Governing equations describing the exhaust manifold dynamics are similar to those describing HCCI combustion dynamics. The following two coupled differential equations describe exhaust manifold dynamics [49]:

$$\dot{m}_{man} = \dot{m}_{in} - \dot{m}_{out} \tag{15}$$

$$\dot{U} = \sum_j m_j h_j + \dot{Q} \tag{16}$$

where $U = m_{man} c_v T_{man} = \frac{1}{\gamma - 1} p_{man} V_{man}$ and $h_j = c_{p,j} T$.

Equations 15 and 16 are coupled with the ideal gas law:

$$p_{man} V_{man} = m_{man} R T_{man} \tag{17}$$

Rearranging Equations 15 and 16 using Equation 17 and neglecting heat transfer gives:

$$\dot{p}_{man} = \frac{\gamma R}{V_{man}}(\dot{m}_{in}T_{in} - \dot{m}_{out}T_{man}) \tag{18}$$

$$\dot{T}_{man} = \frac{T_{man}R}{p_{man}V_{man}c_v}(\bar{c}_p\dot{m}_{in}T_{in} - \bar{c}_p\dot{m}_{out}T_{man} - \bar{c}_v(\dot{m}_{in} - \dot{m}_{out})T_{man}) \tag{19}$$

where γ is the heat capacity ratio and c_p and c_v are the specific heat at constant pressure and volume respectively. The conservation of manifold gas species can be expressed as:

$$\dot{y}_{man} = \sum_j \frac{\dot{m}_j}{m_{man}}(y_j - y_{man}) \tag{20}$$

The adiabatic formulations 18, 19 and 20 estimate the exhaust manifold behavior.

In this study a heater is used to increase the intake manifold temperature to a constant, hence an isothermal assumption is used for intake manifold modeling. Equations 18 and 19 can be simplified [49] to:

$$\dot{p}_{man} = \frac{RT_{man}}{V_{man}}(\dot{m}_{in} - \dot{m}_{out}) \tag{21}$$

$$T_{man} = constant \tag{22}$$

The equation for the conservation of the intake charge species is similar to Equation 20 so it is not repeated here. A one dimensional quasi steady compressible flow model is used to calculate mass flow rates through the intake and exhaust valves during induction and exhaust strokes. The intake and exhaust manifolds are treated as volumes with known pressure, temperature and mixture composition. When reverse flow to the manifolds occurs, a rapid mixing model is used. At each step of the intake or the exhaust strokes, values for the valve open areas are obtained from tabulated data of the actual valve profile. Given the valve open area, the discharge coefficient, and the pressure ratio across a valve, the mass flow rate across the valve is calculated [46] from:

$$\dot{m} = C_d A \frac{P_o}{RT_o} \sqrt{\gamma RT_o}\left(\frac{2}{\gamma-1}\left[\left(\frac{P_s}{P_o}\right)^{\frac{2}{\gamma}} - \left(\frac{P_s}{P_o}\right)^{\frac{\gamma+1}{\gamma}}\right]\right)^{\frac{1}{2}} \tag{23}$$

where C_d is the discharge coefficient, A is the valve open area, P_o is the pressure upstream of the valve, P_s is the pressure downstream of the valve, T_o is the temperature upstream of the valve, γ is the ratio of specific heats and R is the gas constant. For the case of choked flow, Equation 23 reduces [46] to:

$$\dot{m} = C_d A \frac{P_o}{RT_o}\sqrt{\gamma RT_o}\left(\frac{2}{\gamma+1}\right)^{\frac{(\gamma+1)}{2(\gamma-1)}} \tag{24}$$

The throttle is considered as a flow restriction area and Equations 23 and 24 are applied for throttle body simulation.

Engine speed is modeled using a constant engine inertia. The differential equation for engine speed is:

$$I_{eng}\dot{\Omega} = T_{eng} - T_{load} \tag{25}$$

where T_{eng} is engine torque, Ω is engine speed, T_{load} is load torque and I_{eng} is the engine inertia [49].

The state equations for the model are given by Equations 5, 8, 11, 18, 19, 20, 21 and 25. The system under study can be written in the following general form, where x is the state of the system, u is the control input, w is a disturbance, and f is a nonlinear function.

$$\dot{x} = f(t, x, u, w) \tag{26}$$

where $x \in \Re^n$, $u \in \Re^m$ and $w \in \Re^p$. This notation is a vector notation, which allows us to represent the system in a compact form. The main inputs of the model are the intake manifold temperature, valve timing, fuel mass flow rate and the load torque, $u^T = [\dot{m}_f \ T_{int} \ \theta_{IVO} \ \theta_{EVC} \ T_{load}]$. In addition to the inputs, the model also includes certain output variables that can be used to monitor and control the system. These outputs are combustion timing, peak pressure, pressure rise rate and output work, $y^T = [\theta_{SOC} \ P_{max} \ PRR \ W]$. The state variables are chosen due to their physical significance to the combustion process and are: in-cylinder and manifold temperature and pressure, species mass fraction and engine speed, $x^T = [T_{cyl} \ P_{cyl} \ T_{man} \ P_{man} \ y_{man} \ y_{cyl} \ \Omega]$. So for the detailed physical model n=483 [14(zones)×29(species in each zone)+14(temperature at each zone)+1 (in-cylinder pressure) +2(manifolds)×29(species)+2(intake and exhaust manifolds temperatures)+2(intake and exhaust manifolds pressures)] and m=5.

CONTROL ORIENTED MODEL (COM)

Model reduction of the previously described DPM model is used to develop a Control Oriented Model (COM) of a single cylinder HCCI engine. COM is developed based on the approach proposed in [50]. The system of interest is the instantaneous contents of the cylinder. It is assumed that there is no spatial variation in properties within a cylinder at any

instant of time. In order to determine the thermodynamic state of the mixture at IVC, the contents of the in-cylinder mixture must first be determined. The contents of the cylinder at the current cycle *k* depend on fresh reactants inducted during cycle *k* and residual gases from the last cycle, *k* − 1. For lean combustion of n-heptane with internal EGR, the inducted charge becomes:

$$\phi_k C_7H_{16} + c_1(\alpha_{i,k}(c_2 - \phi_{k-1}) + c_2)O_2 + c_3(c_2 + \alpha_{i,k})N_2 + c_4\alpha_{i,k}\phi_{k-1}CO_2 + c_5\alpha_{i,k}\phi_{k-1}H_2O \quad (27)$$

where α_i, ϕ and k represents the residual gas fraction, fuel equivalence ratio and cycle number respectively and c_i are constants listed in Table 1. The values of α_i are obtained from the formation of the energy balance for the cylinder gas over the intake process from IVO to IVC. The fuel equivalence ratio and residual gas fraction are calculated [50, 51] as:

$$\phi_k = \frac{n_{f,k}}{n_{fs,k}} \quad (28)$$

$$\alpha_{i,k} = \frac{A \;\; P_{EVO,k-1}}{A \;\; P_{EVO,k-1} + B \;\; T_{EVO,k-1}} \quad (29)$$

and $n_{f,k}$ is the number of fuel moles, $n_{fs,k}$ is the number of fuel moles for stoichiometric combustion, $P_{EVO,k-1}$ is the pressure at exhaust valve open, and $T_{EVO,k-1}$ is the temperature at exhaust valve open. The factors A and B are:

$$A = V_{EVC,k-1}\Omega M_f T_{int,k} M_{air}$$
$$B = M_{res}P_{int,k}(V_{IVC,k} - V_{IVO,k})\Omega M_{fuel} + c_6 R M_{res}(m_{f,k} - m_{f,k-1})T_{int,k}M_{air}$$

$V_{IVC,k}$ is the in-cylinder volume at IVC, $V_{IVO,k}$ is the in-cylinder volume at inlet valves open, and $T_{int,k}$ is the intake charge temperature.

Temperature at IVC, T_{IVC}, is the temperature of the mixture at the time of inlet valve closing and is calculated as

$$T_{IVC,k} = \frac{C_{2,k}\alpha_{i,k}T_{EVO,k-1} + C_{1,k}T_{int,k}}{C_{1,k} + C_{2,k}\alpha_{i,k}} \quad (30)$$

where

$$C_{1,k} = \phi_k C_{p,C_7H_{16}} + c_1 C_{p,O_2} + c_3 C_{p,N_2}$$
$$C_{2,k} = c_4\phi_{k-1}C_{p,CO_2} + c_5\phi_{k-1}C_{p,H_2O} + c_3 C_{p,N_2} + c_1(c_2 - \phi_{k-1})C_{p,O2}$$

The intake process is assumed to take place at atmospheric pressure as the variable valve timing engine usually operates at wide-open throttle with the valve timing controlling the amount of air.

$$P_{IVC,k} = P_{int,k} \quad (31)$$

The compression of in-cylinder gas made up of fuel, air and residual gas is assumed to be isentropic. This results in the following equations:

$$T_{SOC,k} = \left(\frac{V_{IVC,k}}{V_{SOC,k}}\right)^{\gamma_c - 1} T_{IVC,k} \quad (32)$$

$$P_{SOC,k} = \left(\frac{V_{IVC,k}}{V_{SOC,k}}\right)^{\gamma_c} P_{IVC,k} \quad (33)$$

where γ_c is determined from experimental data. The crank angle of start of combustion is calculated using a simplified Arrhenius equation [50] as:

$$\theta_{SOC,k} = \theta_{IVC} + \frac{K_{th}\Omega}{A} e^{\left(\frac{E_a}{RT_{IVC,k}\left(\frac{V_{IVC,k}}{V_{TDC}}\right)^{\gamma-1}}\right)} \frac{(\alpha_{i,k}(c_7\phi_{k-1} + c_8) + c_7\phi_k + c_8)}{c_1^b(\phi_k)^a(\alpha_{i,k}(c_2 - \phi_{k-1}) + c_2)^b} \left(\frac{RT_{IVC,k}V_{TDC}}{P_{IVC,k}V_{IVC,k}}\right)^{a+b} + \theta_{offset} \quad (34)$$

where the values of *a, b, A,* θ_{offset}, E_a and K_{th} are listed in Table 1.

Based on the correlations developed in [50] and [52] combustion duration, $\Delta\theta$, is calculated as:

$$\Delta\theta_k = c_9 \;\; c_{10}^{\phi_k} \;\; c_{11}^{T_{IVC,k}\left(\frac{V_{IVC,k}}{V_{SOC,k}}\right)^{\gamma-1}} \;\; c_{12}^{\theta_{SOC,k}} \quad (35)$$

Finally, θ_{50}, the crank angle of fifty percent fuel mass fraction burned, is calculated as:

$$\theta_{50,k} = \theta_{SOC,k} + 0.5\Delta\theta_k \quad (36)$$

The first law of thermodynamics is applied to the system to determine the thermodynamic state of the system after combustion. In-cylinder gas temperature after combustion is calculated as:

$$T_{AC,k} = \frac{D_k + (D_{1,k} - N_{1,k}R)T_{2,k} - D_{1,k}c_{14} + D_{2,k}c_{14}}{D_{2,k} - RN_{2,k}} \quad (37)$$

where

$$
\begin{aligned}
D_k &= c_{13} LHV_{C_7H_{16}} \phi_k \\
D_{1,k} &= \phi_k C_{p,C_7H_{16}} + c_1(\alpha_{i,k}(c_2 - \phi_{k-1}) + c_2) C_{p,O2} + \\
&\quad c_3(c_2 + \alpha_{i,k}) C_{p,N_2} + c_4 \alpha_{i,k} \phi_{k-1} C_{p,O2} + c_5 \alpha_{i,k} \phi_{k-1} C_{p,H_2O} \\
D_{2,k} &= c_5(\phi_k + \alpha_{i,k}\phi_{k-1}) C_{p,H_2O} + c_4(\phi_k + \alpha_{i,k}\phi_{k-1}) C_{p,CO_2} + \\
&\quad c_3(c_2 + \alpha_{i,k}) C_{p,N_2} + c_1(c_2 + \alpha_{i,k} - \alpha_{i,k}\phi_{k-1} - \phi_k) C_{p,O_2} \\
N_{1,k} &= \phi_k + c_1(\alpha_{i,k}(c_2 - \phi_{k-1}) + c_2) + c_3(c_2 + \alpha_{i,k}) + \\
&\quad c_4 \alpha_{i,k} \phi_{k-1} + c_5 \alpha_{i,k} \phi_{k-1} \\
N_{2,k} &= c_5(\phi_k + \alpha_{i,k}\phi_{k-1}) + c_4(\phi_k + \alpha_{i,k}\phi_{k-1}) + c_3(c_2 + \alpha_{i,k}) + \\
&\quad c_1(c_2 + \alpha_{i,k} - \alpha_{i,k}\phi_{k-1} - \phi_k)
\end{aligned}
$$

The in-cylinder pressure after combustion is calculated by applying the ideal gas law before and after combustion as:

$$P_{AC} = \frac{N_{2,k}}{N_{1,k}} P_{SOC,k} \frac{T_{AC,k}}{T_{SOC,k}} \tag{38}$$

The rate of pressure rise is calculated from

$$PRR_k = \frac{P_{AC,k} - P_{SOC,k}}{\Delta\theta_k} \tag{39}$$

Rate of pressure rise is required for proper engine control. Large amounts of energy are released during a short period of time in HCCI engines. For this reason, a pressure rise rate threshold is usually determined to keep the combustion noise under a certain level.

The expansion process, which takes place until the opening of the exhaust valve, is assumed to be isentropic. The temperature and pressure of the in-cylinder gas at EVO are calculated as

$$T_{EVO,k} = \left(\frac{V_{AC,k}}{V_{EVO,k}}\right)^{\gamma_e - 1} T_{AC,k} \tag{40}$$

$$P_{EVO,k} = \left(\frac{V_{AC,k}}{V_{EVO,k}}\right)^{\gamma_e} P_{AC,k} \tag{41}$$

Values of all model parameters and constants are listed in Table 1. Those model parameters are determined from the DPM: γ, K_{th}, c_{13} and 0_{offset}. The parameters γ_c and γ_e are determined from experimental data. The parameters: *a, b, A* and E_a are taken directly from [50, 53].

Rewriting the COM in standard form, where *x* is the state of the system, *u* is the control input and *w* is a disturbance.

$$x_{k+1} = f(x_k, u_k, w_k) \tag{42}$$

$$y_k = g(x_k, u_k, w_k) \tag{43}$$

results in the input, the state, the output and the disturbance as:

$$u = \begin{bmatrix} \theta_{IVO} & \theta_{EVC} & \dot{m}_f \end{bmatrix} \tag{44}$$

$$x = \begin{bmatrix} \alpha_i & T_{IVC} & \theta_{SOC} \end{bmatrix} \tag{45}$$

$$w = \begin{bmatrix} \Omega & \phi & T_{int} & P_{EVO} \end{bmatrix} \tag{46}$$

$$y = \theta_{50} \tag{47}$$

Table 1. Model parameters and constants

a	0.25	c_3	41.4
b	1.5	c_4	7
E_a	15098	c_5	8
R	0.8314	c_6	2
K_{th}	2.31×10^{-6}	c_7	4
γ	1.37	c_8	52.4
γ_e	1.34	c_9	2.07×10^{-18}
γ_c	1.32	c_{10}	3.55
A	5.1×10^{11}	c_{11}	0.993
θ_{offset}	85.2	c_{12}	1.16
c_1	11	c_{13}	0.87
c_2	1	c_{14}	298

DPM AND COM VALIDATION

Both the DPM and COM are validated against experimental data from a single cylinder research engine with the specifications listed in Table 2. The simulations are conducted for a range of equivalence ratios and internal EGR levels. The test points that are used for model validation are listed in Table 3.

Figures 1, 2, 3, 4, 5 compare modeled cylinder pressure profiles and the corresponding 300 cycles of averaged experimental cylinder pressure traces. Both COM and DPM match the experimental pressure trace during compression, combustion and expansion. Start of combustion is predicted accurately in each case. The predicted peak pressure is slightly higher for each case and the reason is the combustion efficiency is assumed 100% in simulation. COM and DPM do not consider the effects of low temperature regions, such as crevices. For the DPM, all fourteen zones have high temperatures which result in complete combustion. This can cause prediction deviations of IMEP and thermal efficiency, but the model is still useful as it is able to capture the effects of valve timing. In each of the five cases, DPM predicts the effective compression ratio slightly lower and this causes a discrepancy between DPM and measured cylinder pressure values during compression. The DPM shows a small abrupt pressure increase during compression before the main combustion and this is caused by early heat release due to the

Low Temperature Reactions (LTR). Table 4 compares some more combustion indices i.e. the prediction and measured location of occurrence of the start of combustion and the predicted and measured peak pressure. This table shows that COM and DPM are accurate for control and thermodynamics analysis of HCCI engines. Both COM and DPM are computationally efficient needing 8 ms and 156 sec respectively to simulate an HCCI cycle on a 2.66 GHz Intel PC.

Table 2. Single cylinder research engine specifications [54]

Bore	97 mm
Stroke	88.9 mm
Compression ratio	13.9:1
Connecting rod length	159 mm
IVO [bTDC]	280
IVC [bTDC]	180
EVO [bTDC]	-180
EVC [bTDC]	-280

Table 3. Operating Conditions for Validation

Case Name	A	B	C	D	E
EVC [bTDC]	-300	-330	-320	-320	-300
IVO [bTDC]	300	330	290	300	320
Ω [RPM]	798	799	800	801	803
ϕ	0.37	0.33	0.36	0.33	0.33
T_{int} [C]	80	80	80	78.9	78.4
P_{int} [Bar]	0.88	0.88	0.88	0.89	0.89

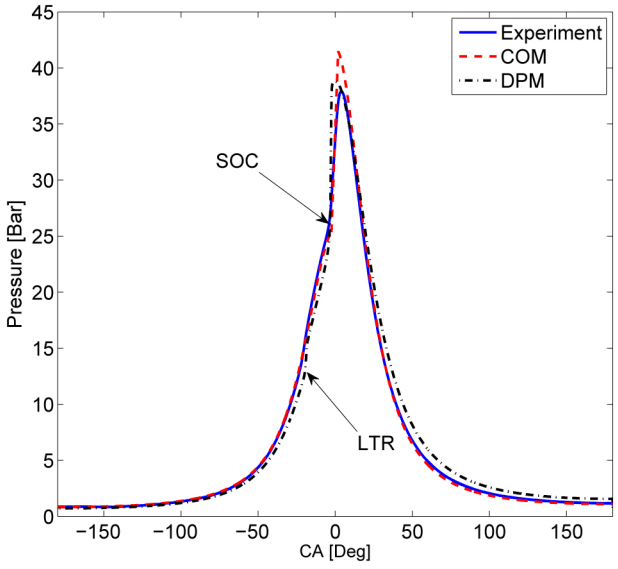

Figure 1. Experiment Pressure Trace vs. Models - Case A (see Table 3)

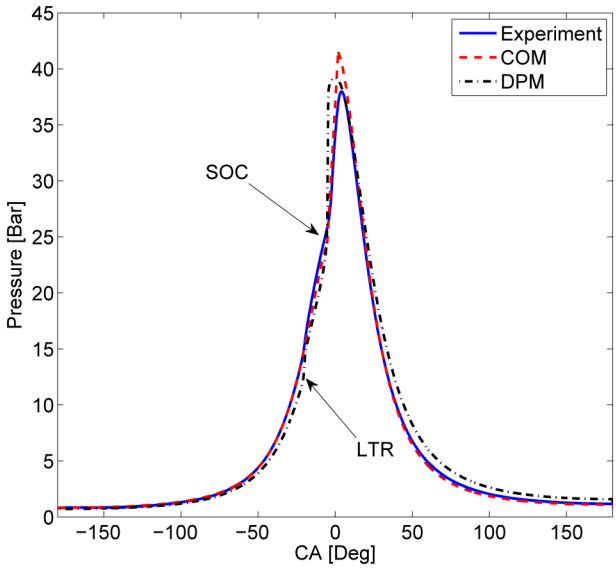

Figure 2. Experiment Pressure Trace vs. Models - Case B (see Table 3)

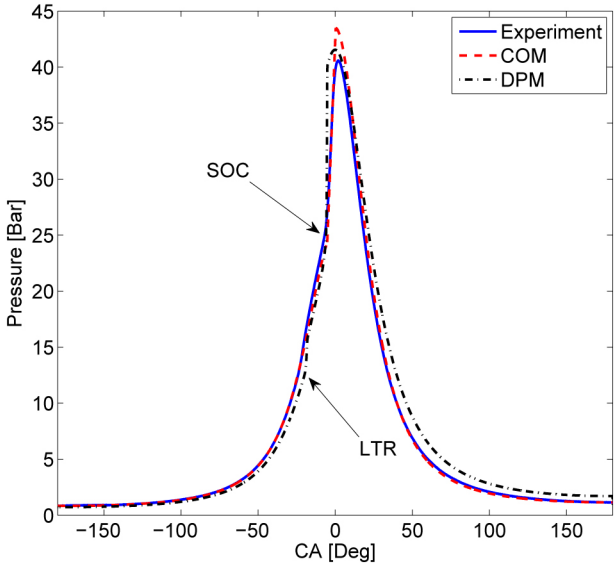

Figure 3. Experiment Pressure Trace vs. Models - Case C (see Table 3)

To further validate both COM and DPM, more experimental data is used. Figure 6 shows predicted and measured θ_{50} when IVO timing changes while holding all other parameters constant. COM and DPM predictions are all within 1-3 crankangle degrees of the measured values. As shown in Figure 6, combustion timing advances when IVO timing is retarded. When IVO is retarded, in-cylinder gas temperature is reduced due to expansion but more fresh charge is inducted into the cylinder due to low in-cylinder pressure at IVO. Mixture composition has key role on HCCI combustion phasing control in this case and combustion advances because the trapped charge fuel equivalence ratio is increased by late IVO. Figure 7 shows predicted and measured θ_{50} when EVC timing changes while keeping other operating parameters

constant. As shown in Figure 7, COM and DPM predictions are acceptable. Combustion timing retards when EVC timing is advanced. When EVC is advanced, in-cylinder gas temperature is increased because more residual gas is trapped but since the pressure is high at IVO part of the residual gas goes into the intake manifold and dilutes the fresh charge. Combustion timing retards because the trapped charge fuel equivalence ratio is reduced by advanced EVC. COM has been further validated in [55].

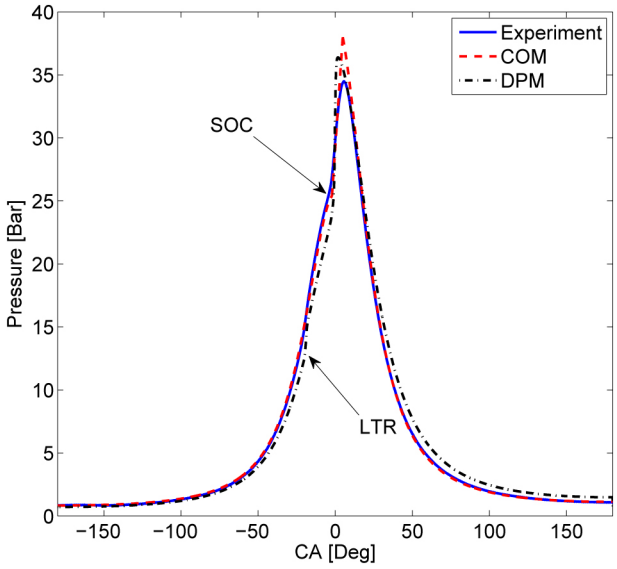

Figure 4. Experiment Pressure Trace vs. Models - Case D (see Table 3)

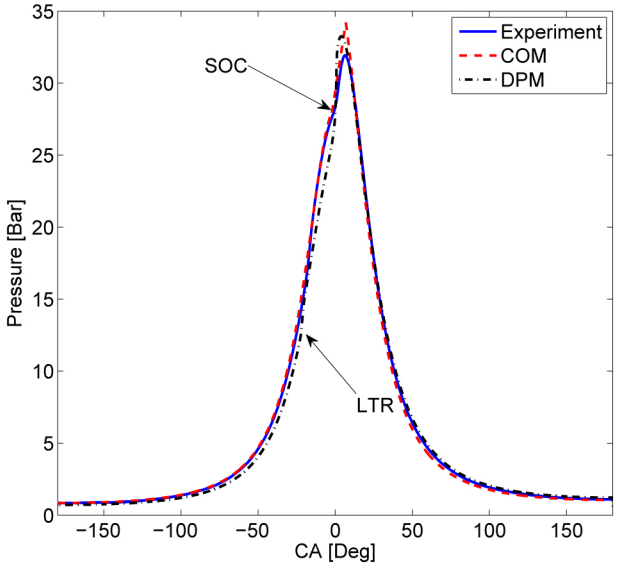

Figure 5. Experiment Pressure Trace vs. Models - Case E (see Table 3)

Table 4. Comparison of predicted and experimental values of peak pressure and start of combustion

Case Name	A	B	C	D	E
Measured SOC [CA aTDC]	-4.3	-6.2	-6.5	-3.7	-0.1
Measured P_{max} [Bar]	37.9	38	40.5	34.5	31.9
Measured $\theta_{P_{max}}$ [CA aTDC]	4	4	1.9	5.6	6.1
DPM SOC [CA aTDC]	-3.8	-5.8	-6.2	-2.2	-0.8
DPM P_{max} [Bar]	38.8	39.2	41.5	36.4	33.26
DPM $\theta_{P_{max}}$ [CA aTDC]	0	-0.1	-0.1	1.9	4
COM SOC [CA aTDC]	-2.4	-5.1	-5.2	-2.1	-1.9
COM P_{max} [Bar]	41.5	41.6	43.5	38	34.2
COM $\theta_{P_{max}}$ [CA aTDC]	1.9	1.8	0.4	4.9	6.9

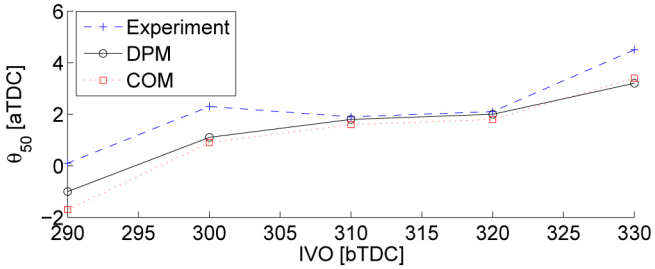

(a). Injected Fuel Energy = 0.36 kJ

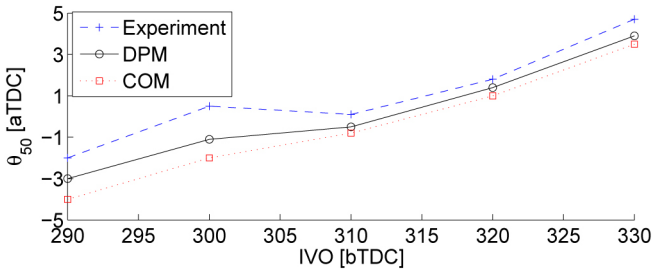

(b). Injected Fuel Energy = 0.39 kJ

Figure 6. Comparison of predicted and measured θ_{50} for IVO timing changes for two injected fuel energy levels (EVC=−320 bTDC, T_{int}=88°C, P_{int}=0.88 Bar and Ω=819 RPM)

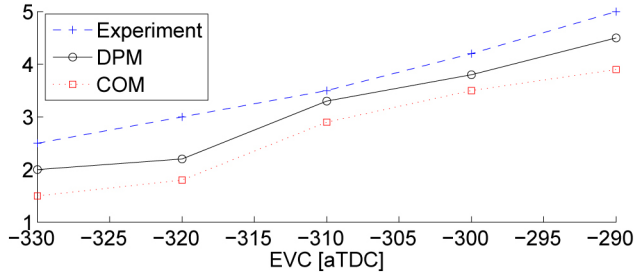

(a). Injected Fuel Energy = 0.36 kJ

Figure 7. Comparison of predicted and measured θ_{50} for EVC timing changes for two injected fuel energy levels (IVO=320 bTDC, T_{int}=88°C, P_{int}=0.88 Bar and Ω=819 RPM)

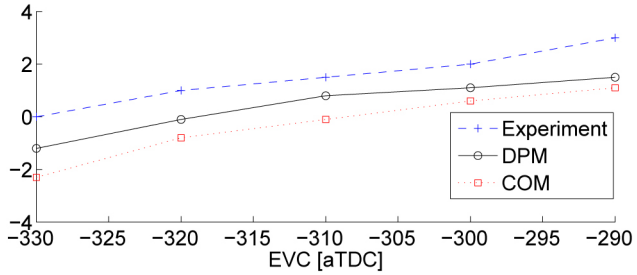

(b). Injected Fuel Energy = 0.39 kJ

Figure 7. (cont.) Comparison of predicted and measured θ_{50} for EVC timing changes for two injected fuel energy levels (IVO=320 bTDC, T_{int}=88°C, P_{int}=0.88 Bar and Ω=819 RPM)

IMPLEMENTATION OF A VARIABLE VALVE TIMING STRATEGY WITH COM AND DPM

VVT is a useful technology for development of HCCI engines [56, 57, 58]. HCCI combustion control with internal EGR is one effective way to avoid misfire at low load and knock at high load. The COM and DPM are used to study the effect of variable valve timing on HCCI combustion. Symmetric Negative Valve Overlap (SNVO) is used as a VVT strategy. This strategy involves early closing of the exhaust valves followed by late intake valve opening. Figure 8a shows a typical pressure trace diagram of HCCI engine with SNVO from the DPM. In Figure 8b, the pressure trace around TDC of combustion is scaled to show more clearly important HCCI combustion indices.

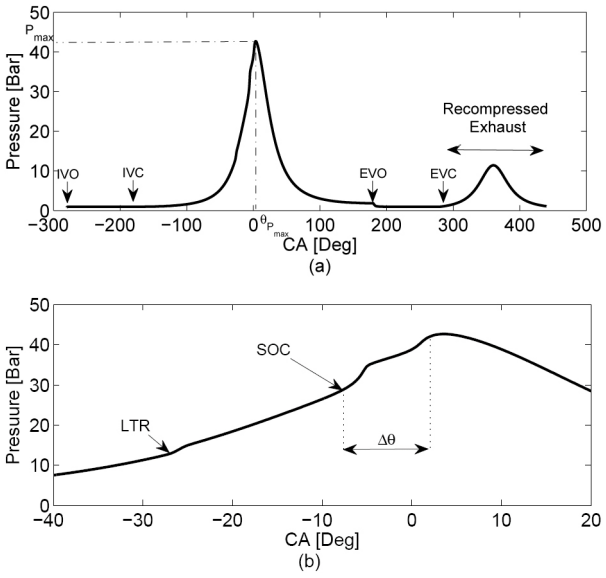

Figure 8. Simulated Pressure Trace of HCCI engine with 160 Deg SNVO (Ω=825 RPM, ϕ=0.3)

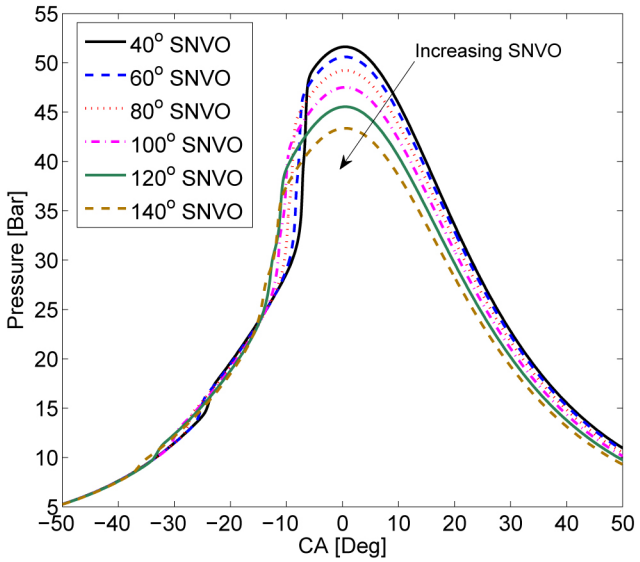

Figure 9. DPM Simulated Pressure Trace of HCCI engine with variable SNVO (Ω=825 RPM)

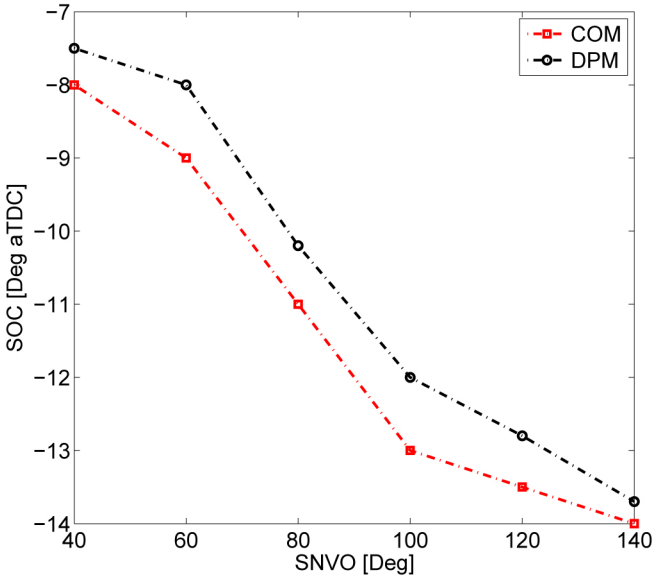

Figure 10. DPM and COM Simulated SOC with variable SNVO (Ω=825 RPM)

As shown in Figure 8a, EVC and IVO timing changes are symmetric around TDC so the recompression work can be regained as expansion work. Six cases are examined, for which SNVO is 40, 60, 80, 100, 120 and 140 degrees. The fueling rate, intake manifold temperature and engine speed are held constant and only the valve timing is changed. DPM and COM simulation results are shown in Figures 9 - 10. Figure 9 shows the in-cylinder pressure from DPM and Figure 10 shows the crank angle of SOC from COM and DPM. When SNVO increases, the amount of internal EGR as well as the in-cylinder gas temperature increases. EGR dilutes the in-cylinder mixture leading to a lower equivalence ratio. SOC is advanced when the in-cylinder gas temperature increases with larger amounts of internal EGR but the peak

pressure is reduced and the combustion duration increases due to lower equivalence ratio of the trapped mixture. These results are consistent with [56].

CONCLUSION

A detailed multi-zone HCCI model (DPM) along with a control oriented model (COM) have been developed and implemented in a full cycle simulation of an HCCI engine for the purpose of predicting and controlling HCCI combustion characteristics. A validation of the both the DPM and COM against experiments in a single cylinder research engine have been conducted over a range of engine loads and valve timings. Comparison of DPM and COM performance with available experimental data shows good agreement. VVT modulates the internal EGR and is one effective way for HCCI combustion timing control. Use of a symmetric negative valve overlap strategy is investigated with both DPM and COM. A wide range of internal EGR can be obtained with this VVT strategy. Ignition timing is advanced and peak in-cylinder pressure is lowered by higher symmetric negative valve overlap durations. In future work, both COM and DPM will be validated against experimental data for other operating ranges.

REFERENCES

1. Zhao H.. *HCCI and CAI engines for the automotive industry*. CRC Press, 2006.

2. Najt, P. and Foster, D., "Compression-Ignited Homogeneous Charge Combustion," SAE Technical Paper 830264, 1983, doi: 10.4271/830264.

3. Atkins M. J. and Koch C. R.. The effect of fuel octane and diluent on HCCI combustion. *Proc. IMechE, Part D*, 219:665 - 675, 2005.

4. Kirchen P. N., Shahbahkti M., and Koch C. R.. A skeletal kinetic mechanism for PRF combustion in HCCI engines. *Combustion Science and Technology*, 179:1059-1083, 2007.

5. Christensen, M. and Johansson, B., "Influence of Mixture Quality on Homogeneous Charge Compression Ignition," SAE Technical Paper 982454, 1998, doi: 10.4271/982454.

6. Martinez-Frias, J., Aceves, S., Flowers, D., Smith, J. et al., "Equivalence Ratio-EGR Control of HCCI Engine Operation and the Potential for Transition to Spark-Ignited Operation," SAE Technical Paper 2001-01-3613, 2001, doi: 10.4271/2001-01-3613.

7. Olsson, J., Tunestål, P., and Johansson, B., "Closed-Loop Control of an HCCI Engine," SAE Technical Paper 2001-01-1031, 2001, doi:10.4271/2001-01-1031.

8. Olsson, J., Tunestål, P., Ulfvik, J., and Johansson, B., "The Effect of Cooled EGR on Emissions and Performance of a Turbocharged HCCI Engine," SAE Technical Paper 2003-01-0743, 2003, doi:10.4271/2003-01-0743.

9. Zhao, H., Peng, Z., Williams, J., and Ladommatos, N., "Understanding the Effects of Recycled Burnt Gases on the Controlled Autoignition (CAI) Combustion in Four-Stroke Gasoline Engines," SAE Technical Paper 2001-01-3607, 2001, doi:10.4271/2001-01-3607.

10. Koopmans, L. and Denbratt, I., "A Four Stroke Camless Engine, Operated in Homogeneous Charge Compression Ignition Mode with Commercial Gasoline," SAE Technical Paper 2001-01-3610, 2001, doi:10.4271/2001-01-3610.

11. Law, D., Kemp, D., Allen, J., Kirkpatrick, G. et al., "Controlled Combustion in an IC-Engine with a Fully Variable Valve Train," SAE Technical Paper 2001-01-0251, 2001, doi:10.4271/2001-01-0251.

12. Li, J., Zhao, H., Ladommatos, N., and Ma, T., "Research and Development of Controlled Auto-Ignition (CAI) Combustion in a 4-Stroke Multi-Cylinder Gasoline Engine," SAE Technical Paper 2001-01-3608, 2001, doi: 10.4271/2001-01-3608.

13. Christensen, M., Hultqvist, A., and Johansson, B., "Demonstrating the Multi Fuel Capability of a Homogeneous Charge Compression Ignition Engine with Variable Compression Ratio," SAE Technical Paper 1999-01-3679, 1999, doi:10.4271/1999-01-3679.

14. Ryan, T., Callahan, T., and Mehta, D., "HCCI in a Variable Compression Ratio Engine-Effects of Engine Variables," SAE Technical Paper 2004-01-1971, 2004, doi: 10.4271/2004-01-1971.

15. Strandh, P., Bengtsson, J., Johansson, R., Tunestål, P. et al., "Cycle-to-Cycle Control of a Dual-Fuel HCCI Engine," SAE Technical Paper 2004-01-0941, 2004, doi: 10.4271/2004-01-0941.

16. Audet, A. and Koch, C., "Actuator Comparison for Closed Loop Control of HCCIC Combustion Timing," SAE Technical Paper 2009-01-1135, 2009, doi: 10.4271/2009-01-1135.

17. Ghazimirsaied A. and Koch C. R.. Controlling cyclic combustion timing variations using a symbol-statistics predictive approach in an HCCI engine. *Applied Energy*, 92(0):133 - 146, 2012.

18. Urushihara, T., Hiraya, K., Kakuhou, A., and Itoh, T., "Expansion of HCCI Operating Region by the Combination of Direct Fuel Injection, Negative Valve Overlap and Internal Fuel Reformation," SAE Technical Paper 2003-01-0749, 2003, doi:10.4271/2003-01-0749.

19. Jang, J., Yang, K., Yeom, K., Bae, C. et al., "Improvement of DME HCCI Engine Performance by Fuel Injection Strategies and EGR," *SAE Int. J. Fuels Lubr.* 1(1): 1075-1083, 2009, doi:10.4271/2008-01-1659.

20. Christensen, M. and Johansson, B., "Homogeneous Charge Compression Ignition with Water Injection," SAE Technical Paper 1999-01-0182, 1999, doi: 10.4271/1999-01-0182.

21. Iwashiro, Y., Tsurushima, T., Nishijima, Y., Asaumi, Y. et al., "Fuel Consumption Improvement and Operation Range

Expansion in HCCI by Direct Water Injection," SAE Technical Paper 2002-01-0105, 2002, doi: 10.4271/2002-01-0105.

22. Milovanovic, N., Chen, R., and Turner, J., "Influence of the Variable Valve Timing Strategy on the Control of a Homogeneous Charge Compression (HCCI) Engine," SAE Technical Paper 2004-01-1899, 2004, doi: 10.4271/2004-01-1899.

23. Bidarvatan, M., Shahbakhti, M., and Jazayeri, S., "Model-Based Control of Combustion Phasing in an HCCI Engine," *SAE Int. J. Engines* 5(3):1163-1176, 2012, doi: 10.4271/2012-01-1137.

24. Millet, J., Maroteaux, F., Emery, P., and Sorine, M., "A Reduced Model of HCCI Combustion in View of Application to Model Based Engine Control Systems," SAE Technical Paper 2006-01-3297, 2006, doi:10.4271/2006-01-3297.

25. Blom, D., Karlsson, M., Ekholm, K., Tunestål, P. et al., "HCCI Engine Modeling and Control using Conservation Principles," SAE Technical Paper 2008-01-0789, 2008, doi: 10.4271/2008-01-0789.

26. Zhou, N., Xie, H., Li, N., Chen, T. et al., "Study on Layered Close Loop Control of 4-Stroke Gasoline HCCI Engine Equipped with 4VVAS," SAE Technical Paper 2008-01-0791, 2008, doi:10.4271/2008-01-0791.

27. Kongsereeparp P.. *Chemical kinetic based simulation for an HCCI engine and its combustion*. PhD thesis, University of Alberta, 2008.

28. Felsch, C., Sloane, T., Han, J., Barths, H. et al., "Numerical Investigation of Recompression and Fuel Reforming in a SIDI-HCCI Engine," SAE Technical Paper 2007-01-1878, 2007, doi:10.4271/2007-01-1878.

29. Szybist, J., McFarlane, J., and Bunting, B., "Comparison of Simulated and Experimental Combustion of Biodiesel Blends in a Single Cylinder Diesel HCCI Engine," SAE Technical Paper 2007-01-4010, 2007, doi: 10.4271/2007-01-4010.

30. Fiveland, S. and Assanis, D., "Development and Validation of a Quasi-Dimensional Model for HCCI Engine Performance and Emissions Studies Under Turbocharged Conditions," SAE Technical Paper 2002-01-1757, 2002, doi: 10.4271/2002-01-1757.

31. Jia, M., Xie, M., and Peng, Z., "A Comparative Study of Multi-zone Combustion Models for HCCI Engines," SAE Technical Paper 2008-01-0064, 2008, doi: 10.4271/2008-01-0064.

32. Babajimopoulos, A., Lavoie, G., and Assanis, D., "Modeling HCCI Combustion With High Levels of Residual Gas Fraction - A Comparison of Two VVA Strategies," SAE Technical Paper 2003-01-3220, 2003, doi: 10.4271/2003-01-3220.

33. Fitzgerald, R., Steeper, R., Snyder, J., Hanson, R. et al., "Determination of Cycle Temperatures and Residual Gas Fraction for HCCI Negative Valve Overlap Operation," *SAE Int. J. Engines* 3(1):124-141, 2010, doi: 10.4271/2010-01-0343.

34. Bastawissi, H., Yu-Sheng, Z., Elkelawy, M., and Bastawissi, A., "Detailed 3D-CFD/Chemistry of CNG-Hydrogen Blend in HCCI Engine," SAE Technical Paper 2010-01-0165, 2010, doi:10.4271/2010-01-0165.

35. Li, G., Bo, T., Chen, C., and Johns, R., "CFD Simulation of HCCI Combustion in a 2-Stroke DI Gasoline Engine," SAE Technical Paper 2003-01-1855, 2003, doi: 10.4271/2003-01-1855.

36. Ohyama, Y., "Air/Fuel Ratio and Residual Gas Fraction Control Using Physical Models for Engines with Widely Variable Valve Timing," SAE Technical Paper 2002-01-2174, 2002, doi:10.4271/2002-01-2174.

37. Shaver G. M., Gerdes J. C., Roelle M. J., Catton P. A., and Christopher F. E.. Dynamic modeling of residual-affected homogeneous charge compression ignition engines with variable valve actuation. *Journal of Dynamics System, Measurement, and Control*, 127:374 -381, 2005.

38. Ogink, R. and Golovitchev, V., "Gasoline HCCI Modeling: Computer Program Combining Detailed Chemistry and Gas Exchange Processes," SAE Technical Paper 2001-01-3614, 2001, doi:10.4271/2001-01-3614.

39. Rausen D. J., Stefanopoulou A. G., Kang J.M., Eng J. A., and Kuo T. W.. A mean-value model for control of homogeneous charge compression ignition (HCCI) engines. *Journal of Dynamics System, Measurement, and Control*, 127:355 -362, 2005.

40. http://www.sandia.gov/chemkin/docs/SENKINabs.html.

41. https://www.avl.com/web/ast/boost.

42. Karagiorgis S., Collings N., Glover K., and Petridis T.. Dynamic modeling of combustion and gas exchange processes for controlled auto-ignition engines. *Proceedinds of the 2006 American Control Conference*, pages 1880 -1885, 2006.

43. Shahbakhti, M. and Koch, C., "Dynamic Modeling of HCCI Combustion Timing in Transient Fueling Operation," *SAE Int. J. Engines* 2(1):1098-1113, 2009, doi: 10.4271/2009-01-1136.

44. http://www.erc.wisc.edu/chemicalreaction.php.

45. https://www-pls.llnl.gov.

46. Assanis D. N.. *Turbocharged Turbocompounded diesel engine system for studies of low heat rejection engine performance*. PhD thesis, Massachusetts Institue of Technology, 1985.

47. Goodwin D. G.. *Cantera C_{++} User's Guide*. California Institute of Technology, 2002.

48. Souder J.S.. *Closed-Loop Control of a Multi-Cylinder HCCI Engine*. PhD thesis, University of California, Berkeley, 2004.

49. Guzzella L.. *Introduction to modeling and control of internal combustion engine systems*. Springer, 2004.

50. Bettis J. B.. Thermodynamic based modelling for nonlinear control of combustion phasing in HCCI engines. Master's thesis, Missouri University of Science and Technology, 2010.

51. Kocher L., Koeberlein E., Alstine D. G. Van, Stricker K., and Shaver G.. Physically based volumetric efficiency model for diesel engines utilizing variable intake valve actuation. *International Journal of Engine Research*, 13:169 -184, 2012.

52. Chiang C.J. and Stefanopoulou A.G.. Sensitivity analysis of combustion timing and duration of homogeneous charge compression ignition (HCCI) engines. In *American Control Conference, 2006*, page 6 pp., June 2006.

53. Warnatz J., Maas U., and Dibble Robert. W.. *Combustion: physical and chemical fundamentals, modeling and simulation, experiments, pollutant formation*. Springer Press, 2006.

54. Seethaler, R., Koch, C., Chladny, R., and Mashkournia, M., "Closed Loop Electromagnetic Valve Actuation Motion Control on a Single Cylinder Engine," SAE Technical Paper 2013-01-0594, 2013, doi:10.4271/2013-01-0594.

55. Ebrahimi K. and Koch C. R.. HCCI combustion timing control with variable valve timing. *Submitted for the American Control Conference*, 2013.

56. Babajimopoulos, A., Assanis, D., and Fiveland, S., "An Approach for Modeling the Effects of Gas Exchange Processes on HCCI Combustion and Its Application in Evaluating Variable Valve Timing Control Strategies," SAE Technical Paper 2002-01-2829, 2002, doi: 10.4271/2002-01-2829.

57. Guohong, T., Zhi, W., Jianxin, W., Shijin, S. et al., "HCCI Combustion Control by Injection Strategy with Negative Valve Overlap in a GDI Engine," SAE Technical Paper 2006-01-0415, 2006, doi:10.4271/2006-01-0415.

58. Johansson, T., Johansson, B., Tunestål, P., and Aulin, H., "HCCI Operating Range in a Turbo-charged Multi Cylinder Engine with VVT and Spray-Guided DI," SAE Technical Paper 2009-01-0494, 2009, doi:10.4271/2009-01-0494.

NOMENCLATURE

SYMBOLS

A	Area	[m^2]
θ_{50}	Crank angle for 50% burnt fuel	[CAD aTDC]
C_d	Discharge coefficient	[-]
c_v	Constant-volume heat capacity	[$\frac{kJ}{kg.K}$]
c_p	Constant-pressure heat capacity	[$\frac{kJ}{kg.K}$]
$\Delta\theta$	Combustion duration	[CAD]
EGR	Fraction of exh. gas recirculated	[-]
m	Mass	[kg] or [g]
Ω	Engine speed	[rpm]
ϕ	Equivalence ratio	[-]
T	Temperature	[K] or [C]
θ	Crank angle	[CAD]
U	Internal energy	[kJ]
V	Volume	[m^3]
P	Pressure	[Bar]
M	Molecular weight	[kg]
W	Displacement work	[kJ]
y	Mass fraction	[-]

ABBREVIATIONS

aTDC	after Top Dead Center
CAD	Crank Angle Degree
CFD	Computational Fluid Dynamics
CI	Compression Ignition
SNVO	Symmetric Negative Valve Overlap
DPM	Detailed Physical Model
COM	Control Oriented Model
LTR	Low Temperature Reactions

ISSN 0148-7191

SAE Customer Service:
Tel: 877-606-7323 (inside USA and Canada)
Tel: 724-776-4970 (outside USA)
Fax: 724-776-0790
Email: CustomerService@sae.org
SAE Web Address: http://www.sae.org
Printed in USA